Fourth Semiannual Progress Report
to
the National Aeronautics and Space Administration
on
the TM Project

"UTILIZING REMOTE SENSING OF THEMATIC MAPPER DATA TO IMPROVE OUR UNDERSTANDING OF ESTUARINE PROCESSES AND THEIR INFLUENCE ON THE PRODUCTIVITY OF ESTUARINE-DEPENDENT FISHERIES"

Joan A. Browder
Southeast Fisheries Center
National Marine Fisheries Service
75 Virginia Beach Drive
Miami, Florida 33149

L. Nelson May, Jr.
Coastal Fisheries Institute
Center for Wetland Resources
Louisiana State University
Baton Rouge, Louisiana 70803

Alan Rosenthal
Southeast Fisheries Center
National Marine Fisheries Service
75 Virginia Beach Drive
Miami, Florida 33149

Robert H. Baumann
Center for Energy Studies
Louisiana State University
Baton Rouge, Louisiana 70803

James G. Gosselink
Coastal Ecology Institute
Center for Wetland Resources
Louisiana State University
Baton Rouge, Louisiana 70803

June 10, 1987

INTRODUCTION

A stochastic spatial computer model addressing coastal resource problems in Louisiana is being refined and validated using thematic mapper (TM) imagery. Investigators at the Southeast Fisheries Center, National Marine Fisheries Service (NMFS), in Miami and at Louisiana State University's Center for Wetland Resources and Center for Energy Studies in Baton Rouge are participating in the research, which consists of two major activities:

1. Measuring land (or emergent vegetation) and water and the length of the interface between land and water in TM imagery of selected coastal wetlands (sample marshes)

2. Comparing spatial patterns of land and water in the sample marshes of the imagery to those in marshes simulated by the computer model

We completed a significant amount of work during the fourth semiannual period. This report discusses our accomplishments in modeling by the NMFS group and in digital processing of TM data by the LSU group. Planned future work is briefly discussed in a final section.

LSU activities during the fourth semiannual period focused on preprocessing TM images of brackish marsh sites and tabulating data on spatial parameters from TM images of the salt marsh sites. We continued to use the Fisheries Image Processing System (FIPS) maintained by NMFS in Slidell, Louisiana, to analyze the TM scene. FIPS uses a Sperry-Univac V77/600 computer, color image display device, and other hardware to process remotely sensed digital imagery. The software is a modified version of the Earth

Resources Laboratory Applications Software (ELAS) (Graham et al. 1984).

NMFS activites were concentrated on improving the structure of the model and developing a structure and methodology for calibrating the model with spatial-pattern data from the TM imagery.

PREPROCESSING OF TM IMAGERY

The study sites were selected during the third semester of the study (see Browder et al. 1986). They are located in salt and brackish marsh areas on two abandoned delta lobes of the Mississippi River located in southern Louisiana. The early Lafourche lobe was an actively prograding delta within the last 1,800 years; the late Lafourche lobe was active as a main distributary of the river within the last 600 years.

We selected salt marsh study sites on each delta lobe that correspond to the boundaries of five contiguous U.S. Geological Survey 7.5-min topographic maps. We then divided the individual topographic maps into four contiguous quarters, each encompassing an area 192 elements wide and 192 scan lines long on the TM image. The intersection of the four quarters was aligned to correspond to the center point of each topographic map. Thus, a total of 40 salt marsh sites, 20 on each delta lobe, were available for the analysis.

TM images of the brackish marsh sites were georeferenced to fit a Universal Transverse Mercator projection with a north-south orientation. The registration technique was identical to the method used to rotate TM images of the salt marsh sites; the ELAS modules PMGC and PMGE were used to accumulate ground-control points, generate polynomial least-squares mapping equations, and resample the image using the bilinear interpolation technique. Registration accuracies for the early and late Lafourche sites were

35 and 22 m, respectively.

We will have fewer brackish marsh sample sites than salt marsh sites because of cloud cover, the upper boundary of the TM scene, the presence of upland areas, and the irregular boundaries of brackish marsh areas. We have estimated that approximately 15–25 brackish marsh sites will be available for the analysis.

TECHNIQUE FOR SEGMENTING TM IMAGES INTO LAND AND WATER

We continued to explore image enhancement and gray-level thresholding techniques for segmenting the TM images into land and water. We visually evalated land and water discrimination in experimental images representing three enhancement techniques: (1) a band-5 image with the shorelines enhanced by high-pass filtering (Moik 1980), (2) a product image generated from bands 4 and 5, and (3) a ratio image derived from bands 3 and 5. The experimental images included the Leeville oil field, an oil and gas field comprising numerous small and linear water bodies such as ponds, lakes, and man-made canals.

The product and ratio images seemed to provide slightly better discrimination of small water bodies than did the edge-enhanced band-5 image. The product and ratio images were approximately equal in their ability to discriminate shorelines in the test area; the product image, however, had an advantage over the ratio image because the effects of multiplying bands 4 and 5 seemed to reduce the number of noisy pixels in open-water areas and thus eliminated the need to digitally mask these areas. A product image including all of the study sites was then generated and rescaled for a 0–255 display.

We used the entropic thresholding technique described by Pun (1981) to segment the product image into land and water pixels. This automated technique takes into account the asymmetrical shape of the gray-level histogram to define a threshold between land and water pixels. The threshold is derived from an anisotropic coefficient, which is related to the geometric shape of the gray-level histogram. Pun's method was selected instead of other thresholding techniques (e.g., Kirby and Rosenfield 1979; Weszka and Rosenfield 1978) because it was simple to implement on our system and seemed to provide a reasonable depiction of the land-water ratio in the TM images of the study sites.

TABULATION OF SPATIAL PARAMETER DATA FROM THE TM IMAGES

A total of 40 binary land-water images were generated from the product image of the salt marsh sites. These images were labeled and stored on tape. Algorithms based on sequential ELAS commands were set up for batch processing to generate the data for each of these sites for the spatial model. We measured the following spatial-pattern parameters: (1) total numbers of land and water pixels; (2) total numbers of water pixels by scan line and element column; (3) total number of land-water joins; (4) total number of water pixel sides adjacent to one, two, three, and four other water pixels; and (5) number of pixels by water body size. A significant amount of processing was completed for the salt marsh study sites during this semester of activity (Table 1).

Table 2 lists the percentage of each area that is open water and the number of land-water joins in each of the 40 salt marsh study sites. The percentage of an area that is open water indicates the level of disintegration (i.e., an area that is 40 percent water is disintegrated to the

40 percent level). The number of land-water joins is synonymous with interface and, multiplied by 2, gives the cross-product statistic. A plot of land-water joins, or interface, is given in Figure 1. Two aspects of this plot are worth noting. First, data are missing at the lower end of the scale of marsh disintegration. Fortunately, we expect to obtain data in this range from the brackish marsh sites, which have yet to be processed. Second, the plot suggests that the land-water interface continuously declines with disintegration levels greater than 40 percent. We think that several parabolic curves of interface versus disintegration level may exist in this data, but marsh simulations with models calibrated to these data will be necessary to define the trajectories.

TECHNIQUE TO GENERATE SPATIAL AUTOCORRELATION STATISTICS

Testing was completed on some new ELAS software developed under contract by Delta Data Systems, Inc., of Picayune, Mississippi. The software computes the general cross-product statistic (R), the expected value and variance of R, and a test statistic based on a z-approximation from each binary land-water image derived from the TM data. We are using these parameters to quantify the level of spatial autocorrelation present in the distribution of water bodies in each study site. The software utilizes equations from Upton and Fingleton (1985).

We encountered some Some operational problems with the new software. First, some elaborate modifications were required to accommodate the 16-bit architecture and limited memory of the host computer. These problems, coupled with the complexity of the task, resulted in lengthy execution times. An average of seven days was required to complete the computations

for a single 192-x-192 image. Second, the FIPS computer is not stable enough to complete batch jobs requiring 24 hours or more of execution time. We estimated that about one calendar year would be required to complete the tabulations for the 40 salt marsh study sites, given the lengthy execution times, other demands placed on the system, and the instability of the host computer.

Fortunately, an alternative was available. Upton and Fingleton (1985) provide a second set of equations for calculating R, E(R), and var(R) by means of the number of land pixels, the number of water pixels, and the number of land-water joins (which is equivalent to the length of the land-water interface) of a rectangular or square matrix. These equations are inappropriate for areas of other shapes or those having irregular boundaries; however, they apply perfectly to our square sites. By switching to new algorithms based on these equations, we were able to keep spatial-pattern computations within the range of practicality.

MODEL REFINEMENT AND CALIBRATION

The model has two weighting factors that affect the probability that a given pixel will convert to water at the next iteration and that, therefore, affect the pattern of land and water in the simulated marsh. The first weighting fac tor, W, is related to the number of sides on which each land pixel is bor dered by water pixels. The second probability factor, G, relates to the position of each pixel in the marsh relative to the main water body (in this case, the Gulf of Mexico). As the model originally was written, even when $G > 0$, only those water pixels initially bordering the main water body had heightened probabilities of converting to water. In testing the sen sitivity of this model to the two weighting factors, we

found that G did not appreciably affect the cross-product statistic (R), which we plan to use to calibrate the model to simulate specific marshes from TM imagery. Essentially, we had only one functional weighting factor, W, which might have provided too little latitude for fitting the land-water patterns of our simulated marshes to those of actual marshes.

The parameter R was much more sensitive to variation in G in a second version of the model completed during this semester of activity. In this model, if $G > 0$, pixels throughout the marsh have a higher probability of converting to water if they border on the main water body at any time during the simulation. In sensitivity tests of this model, we found a strong and highly nonlinear relationship of R to G and W. This new version of the model seems to be much more suitable to our needs; although, owing to the nonlinear effect of W and G on R, the task of setting W and G on the basis of R will be more difficult than anticipated. Figure 2 is not sufficiently detailed to provide a thorough representation, but roughly depicts how R varies with respect to G and W in a marsh of 48 x 48 pixels. Each point represents the mean from five simulation runs. Since the execution of even one simulation is fairly slow (see our third semi-annual progress report, Browder et al. 1986), the process of developing such a graph takes several weeks. Because R is dependent upon the size of the marsh and we plan to be working with 192-x-192 samples from the TM imagery, we decided to start at once on a graph of this sort for the larger marsh rather than spending any more time on the graph for the smaller marsh. The graph being prepared will be more detailed and, formatted as a look-up table, will help us select the weighting factors to best approximate the land-water patterns of marshes in the TM imagery.

Using digitized information from a habitat map (Wicker et al 1980), the LSU group tabulated data on spatial-pattern parameters for four 96-x 96-pixel areas within the late Lafourche salt marsh study site. The habitat maps are stored as part of the Map Overlay and Statistical System (MOSS) data base maintained by the U.S. Fish and Wildlife Service. (MOSS digital data converted from a polygon to a cell format were available for our use.) The data were for four subquarters of the northwestern quarter of the Mink Bayou quadrangle. The parameters tabulated were number of land pixels, number of water pixels, number of land-water joins (J), and number of water pixels with sides adjacent to 1 (ADJ-1), 2 (ADJ-2), 3 (ADJ-3), and 4 (ADJ-4) water pixels (Table 3). These were the first data on actual marshes that we had seen, and we used it to gain perspective on fine tuning and calibrating the model before we received any data from the TM imagery.

The four marshes were in slightly different stages of disintegration, ranging from 27 to 57 percent water. For the other spatial-pattern parameters to be exactly comparable, the marshes would have to be at the same disintegration level. Keeping this in mind, we still thought the data suggested some independent variation of the side-adjacency data and J. For instance, the proportion of ADJ-4 pixels seems much higher in the southeastern quarter than in the northeastern quarter and the proportion of 3-ADJ pixels seems much lower in the southeastern quarter than in the northeastern quarter, although the level of disintegration in these two marsh areas is about the same. This suggests that we might need more than one spatial-pattern parameter to set our weighting factors. Furthermore, it confirms our suspicion that two weighting factors should have separate effects. Clearly, the second version of the model is more suitable than the first one.

To further explore the relationship between J and ADJ-1, 2, 3, and 4, we executed 25 simulations (each with five replications) of a 48-x-48 pixel-marsh and, at the 50 percent level of disintegration, collected data on J and ADJ-all. Linear regressions (Table 4) indicated that J and ADJ-4 were highly correlated (R^2 = 0.89) and that over 40 percent of the variation in each of these variables could be explained by W, G, and their product. The numbers of water pixels with 2 and 3 sides adjacent to water were significantly related to only the G weighting factor and, therefore, appear independent of the W weighting factor. The R^2 of the relationship between ADJ-3 and G was higher than that between ADJ-2 and G. All four side-adjacency variables were correlated with interface (Table 5), but the relationship between ADJ-3 and interface was the weakest (R^2 was only 0.27 for ADJ-3, whereas it was 0.95 for ADJ-1, 0.85 for ADJ-2, and 0.89 for ADJ-4.

Several results of these analyses suggested that ADJ-3 would be a good variable to use in combination with R to select the best W and G to simulate the spatial patterns of a given marsh. First, ADJ-3 was significantly related to G but not to W, and ADJ-3 had a stronger relationship with G than did ADJ-2. Secondly, ADJ-3's correlation with R was weaker than that of the other side-adjacency variables; thus, W and G would be selected on the basis of two relatively independent variables.

Tentatively, we plan to select starting values of W and G by developing isopleths of ADJ-3 and a corresponding look-up table to use in conjunction with the R-value look-up table to make our initial W and G selections. By superimposing the two sets of isopleths and determining the point or general area of W and G where contours of the desired R and the desired ADJ-3 intersect or most nearly intersect, we can select the W and G that will best approximate the spatial pattern of land and water in the

sample. It will be necessary to prepare pairs of isopleths (one for R and one for ADJ-3) for five levels of disintegration (0.1, 0.2, 0.3, 0.4, and 0.5) and to interpolate between them to match TM marshes at all possible disintegration levels. Once we have found the general region of W and G by means of the isopleths, we plan to approach the optimal values through an structured iterative decision-making process.

FUTURE ACTIVITIES

During the upcoming semester we will complete all of the tabulations from TM images of the salt marsh study sites and continue processing the brackish marsh study sites. We expect to complete the tabulations of spatial-pattern data on the brackish marsh sites by the end of the semester.

Within the next few weeks we will have collected the necessary data from model simulations needed to construct the isopleths and look-up tables for R and ADJ-3. The next step will be to develop the decision-making procedure to fine-tune our estimates of weighting factors W and G. Then we will begin to select the W's and G's for the salt marsh study sites.

ACKNOWLEDGMENTS

We wish to thank the following persons and organizations for their help during this phase of the project: Deborah A. Fuller, Center for Wetland Resources, Louisiana State University; and Andrew Kemmerer and Gerald Williamson, Mississippi Laboratories, National Marine Fisheries Service.

REFERENCES

Browder, J. A., L. N. May, Jr., Alan Rosenthal, R. H. Baumann, and J. G. Gosselink. 1986. Third semiannual progress report to NASA on the TM project, "Utilizing remote sensing of thematic mapper data to improve our understanding of estuarine processes and their influence on the productivity of estuarine-dependent fisheries." National Marine Fisheries Service, Miami, Fla., and Louisiana State University, Baton Rouge, La. 22 pp.

Graham, M. H., B. G. Junkin, M. T. Kalcic, R. W. Pearson, and B. R. Seyfarth. 1984. ELAS: Earth Resources Laboratory Applications Software, Vol. 2, ELAS User's Guide. NASA Earth Resources Laboratory, NSTL, Miss. 428 pp.

Kirby, R. L., and A. Rosenfeld. 1979. A note on the use of (gray-level, local average gray-level) space as an aid in threshold selection. IEEE Transactions on Systems, Man, and Cybernetics, Vol. SMC-9, No. 12, pp. 860-864.

Moik, J. G. 1980. Digital processing of remotely sensed images. National Aeronautics and Space Administration Scientific and Technical Information Branch, NASA SP-431. 330 pp.

Pun, T. 1981. Entropic thresholding, a new approach. Computer Graphics and Image Processing 16: 210-239.

Upton, G., and B. Fingleton. 1985. Spatial Data Analysis by Example. Vol. 1. New York: Wiley. 410 pp.

Weszka, J. S., and A. Rosenfeld. 1978. Threshold evaluation techniques. Pages 622-629 in IEEE Transactions on Systems, Man, and Cybernetics, Vol. SMC-8, No. 8.

Wicker, K. M., J. B. Johnston, M. W. Young, and R. M. Rogers. 1980. Mississippi deltaic plain region habitat mapping study. 464 maps. U.S. Fish and Wildlife Service, Office of Biological Services. FWS/OBS-79/07.

LIST OF FIGURES

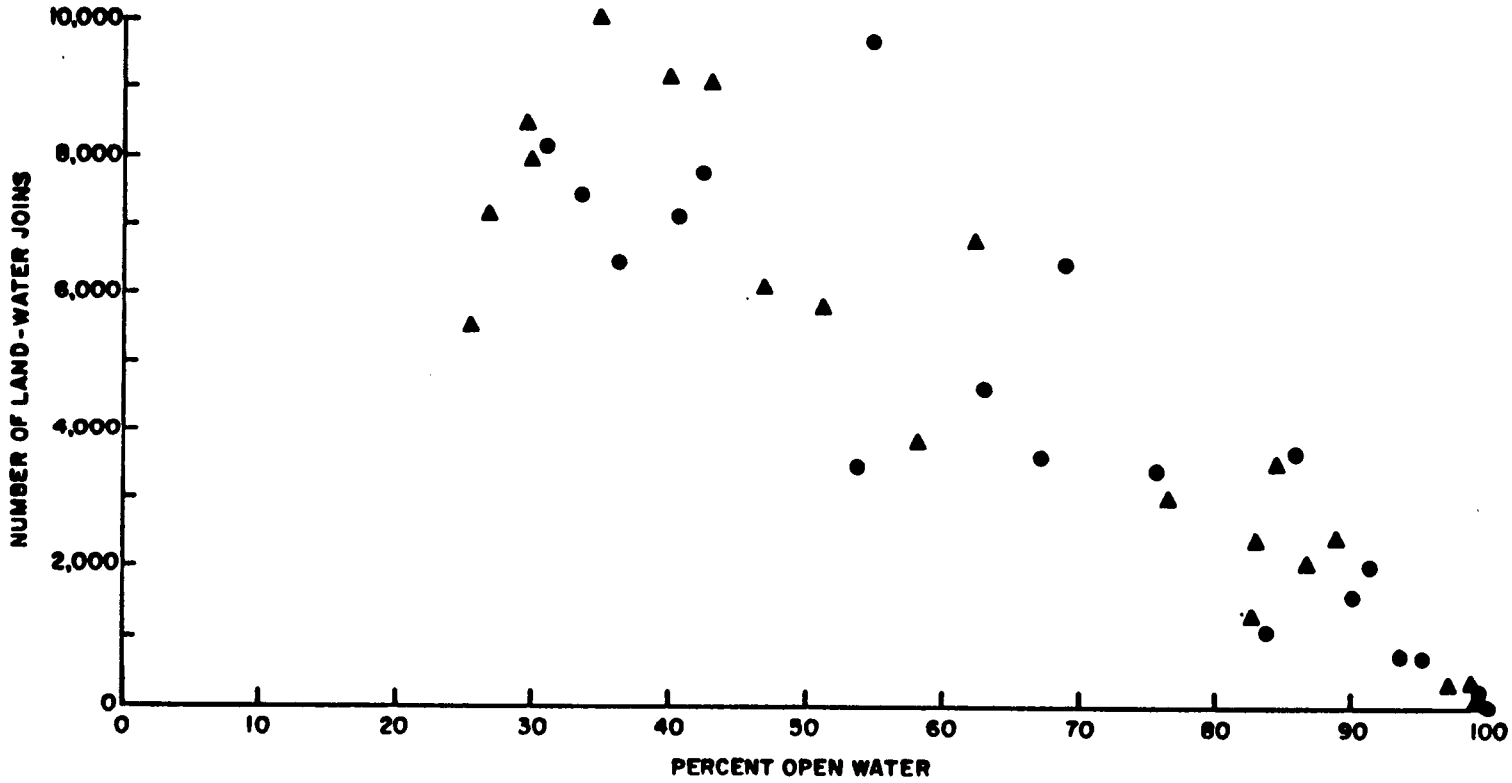

Figure 1. Plot of the number of land-water joins versus the percentage of open-water area derived from the TM images of the 40 salt marsh sample sites.

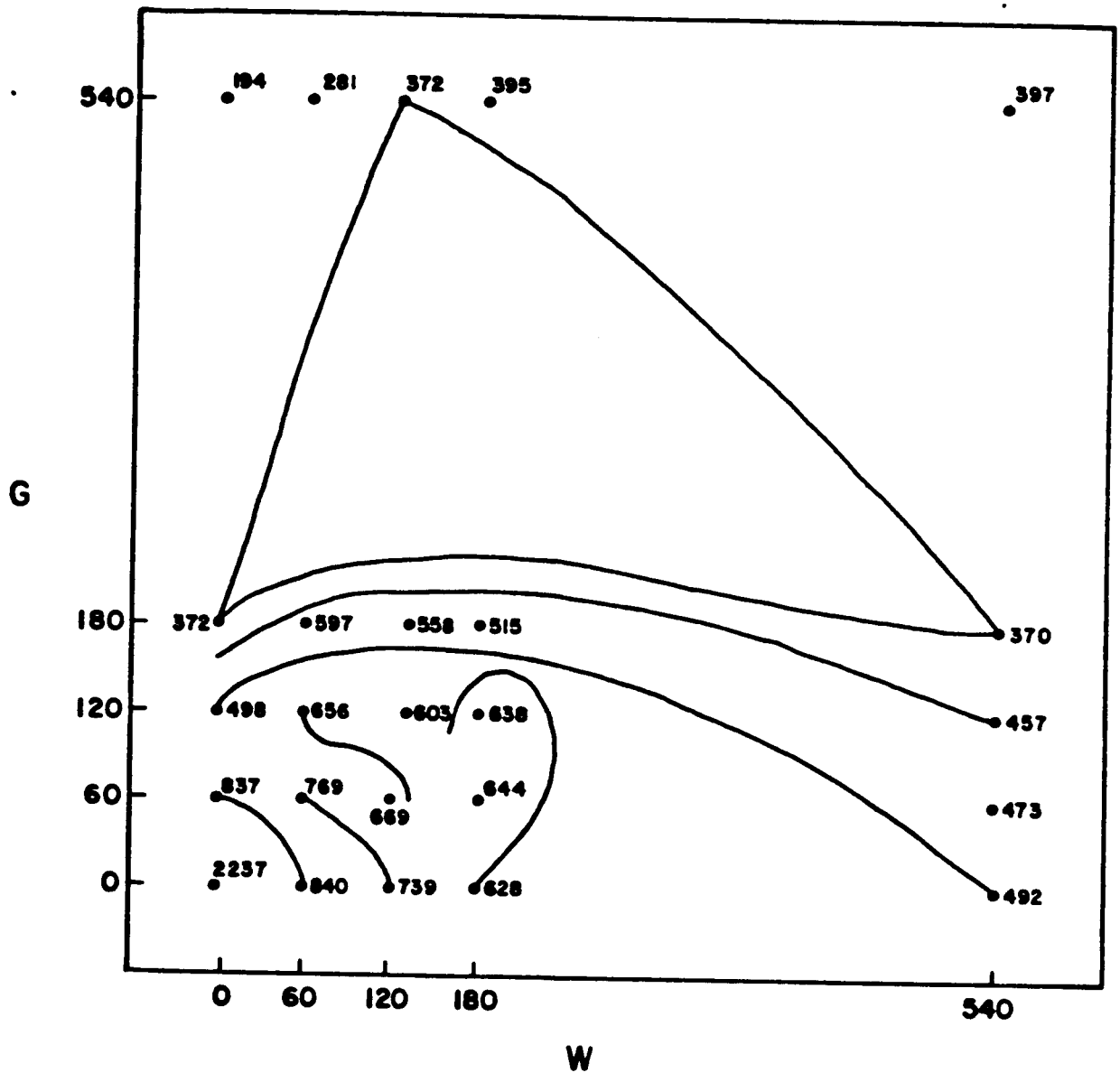

Figure 2. Isopleth plot of the land-water interface as a function of G and W, constructed from mean values of five simulation runs for a 48-x-48-pixel marsh.

Table 1. Progress to date in processing TM imagery (X's indicate completed units).

Quadrangle name	Quar.	Delta lobe [a]	Marsh type [b]	Land-water pixels	Land-water joins	Water pixels				R	E(R)
						By row	By col.	Water adj.	Water body size		
Leeville	NW	L	S	X	X	X	X	X	X		
	NE	L	S	X	X	X	X	X	X		
	SE	L	S	X	X	X	X	X			
	SW	L	S	X	X	X	X	X			
Mink Bayou	NW	L	S	X	X	X	X	X			
	NE	L	S	X	X	X	X	X			
	SE	L	S	X	X	X	X	X			
	SW	L	S	X	X	X	X	X			
Caminada	NW	L	S	X	X	X	X	X			
Pass	NE	L	S	X	X	X	X				
	SE	L	S	X	X	X	X				
	SW	L	S	X	X	X	X				
Bay Tambour	NW	L	S	X	X	X	X				
	NE	L	S	X	X		X				
	SE	L	S	X	X		X				
	SW	L	S	X	X		X				
Pelican	NW	L	S	X	X		X				
Pass	NE	L	S	X	X		X				
	SE	L	S	X	X		X				
	SW	L	S	X	X		X				
Grand Bayou	NW	E	S	X	X		X				
du Large	NE	E	S	X	X		X				
	SE	E	S	X	X		X				
	SW	E	S	X	X		X				
Lake	NW	E	S	X	X		X				
La Graisse	NE	E	S	X	X		X				
	SE	E	S	X	X		X				
	SW	E	S	X	X		X				

(continued)

Table 1. (Continued.)

Quadrangle name	Quar.	Delta lobe [a]	Marsh type [b]	Land-water pixels	Land-water joins	Water pixels				R	E(R)
						By row	By col.	Water adj.	Water body size		
Central Isles Dernieres	NW	E	S	X	X		X				
	NE	E	S	X	X		X				
	SE	E	S	X	X		X				
	SW	E	S	X	X						
Cocodrie	NW	E	S	X	X						
	NE	E	S	X	X						
	SE	E	S	X	X						
	SW	E	S	X	X						
Dog Lake	NW	E	S	X	X						
	NE	E	S	X	X						
	SE	E	S	X	X						
	SW	E	S	X	X						

[a] L = late Lafourche; E = early Lafourche.

[b] S = Salt marsh.

Table 2. Percentage of open water area and number of land-water joins tabulated from TM images of the salt-marsh study sites.

Quadrangle name	Quarter	Percentage water	Number of land-water joins
Leeville	NW	42.939	9,093
	NE	34.926	10,025
	SE	39.912	10,118
	SW	46.742	6,115
Mink Bayou	NW	26.590	7,166
	NE	24.536	5,519
	SE	29.435	8,420
	SW	29.574	7,937
Caminada Pass	NW	62.093	6,778
	NE	82.867	1,341
	SE	99.265	101
	SW	58.019	3,884
Bay Tambour	NW	51.180	5,818
	NE	76.546	3,047
	SE	88.723	2,245
	SW	84.378	3,515
Pelican Pass	NW	98.964	341
	NE	82.598	2,433
	SE	86.683	2,100
	SW	97.244	385
Grand Bayou du Large	NW	53.833	3,431
	NE	67.255	3,621
	SE	40.435	7,174
	SW	83.716	1,111
Lake La Graisse	NW	91.132	2,079
	NE	99.278	292
	SE	100.000	0
	SW	99.997	4
Central Isles Dernieres	NW	75.770	3,439
	NE	90.053	1,605
	SE	95.182	748
	SW	93.533	745
Cocodrie	NW	33.434	7,430
	NE	68.894	6,457
	SE	85.786	3,681
	SW	54.715	9,692
Dog Lake	NW	62.972	4,612
	NE	30.735	8,114
	SE	42.377	7,774
	SW	36.396	6,482

Table 3. Spatial-pattern parameters tabulated from four subquarters of the northwestern quarter of the 1978 Mink Bayou habitat map (Wicker et al. 1980).

Subquarter [a]	No. of land pixels	No. of water pixels	Percentage water	No. of land-water joins	Water pixels by number of sides adjacent to other water pixels			
					1	2	3	4
NW	3,975	5,241	56.87	1,822	66	498	628	4,049
NE	6,735	2,481	26.92	1,942	65	534	679	1,203
SE	6,486	2,730	29.62	1,898	57	613	501	1,559
SW	6,210	3,006	32.62	1,987	39	558	749	1,660

[a] Size: 96 x 96 pixels.

Table 4. Results of the multiple regression of selected spatial-pattern parameters from 25 simulations of a 48-x-48-pixel marsh on probability weighting factors of the model.

Dependent variable	Regression coefficients of the independent variables			Constant	R^2 [a]	SE of estimate	Sig. F
	W	G	W X G				
L-W Joins	-1.09141	-1.53730	0.00313	983.59248	0.41422	309.35	0.0094
SE	0.44948	0.44948	0.00172	117.55361	0.33053		
Sig. T	(0.0242)	(0.0026)	(0.0826)	(0.0000)			
2-ADJ		-0.16651		137.7444	0.2005	65.77	0.0248
SE		0.06933		18.13118	0.16577		
Sig. T		(0.0248)		(0.0000)			
3-ADJ		-0.24769		217.98880	0.38479	61.95	0.0009
SE		0.06531		17.07962	0.35804		
Sig. T		(0.0009)		(0.0000)			
4-ADJ	0.41324	0.76386	-0.00149	559.74664	0.43700	138.27	0.0063
SE	0.20091	0.20091	0.0007682	52.54419	0.35657		
Sig. T	(0.0523)	(0.0010)	(0.0655)	(0.0000)			

[a] The second value in each set of R^2 is adjusted R^2.

Note: L-w joins = number of land-water joins.
ADJ-1 = number of water pixels bordered on one side by another water pixels.
ADJ-2 = number of water pixels bordered on two sides by other water pixels.
ADJ-3 = number of water pixels bordered on three sides by other water pixels.
ADJ-4 = number of water pixels bordered on four sides by other water pixels.

Table 5. Results of a simple linear regression of the side-adjacency variables on the land-water interface.

Dependent variable	Regression coefficient (interface)	Constant	R^2 [a]	SE of estimate	Sig. F
ADJ-1	0.12221	-25.97183	0.95351	10.42236	0.0000
SE	0.00563	4.02513	(0.95149)		
Sig. T	(0.0000)	(0.0000)			
ADJ-2	0.17564	0.29345	0.85045	28.44528	0.0000
SE	0.01536	10.98562	(0.84395)		
Sig. T	(0.0000)				
ADJ-3	0.10706	107.89119	0.27401	67.30131	0.0072
SE	0.03634	25.99189	(0.24245)		
Sig. T	(0.0072)	(0.0004)			
ADJ-4	-0.43045	986.66296	0.89131	58.05365	0.0000
SE	0.03134	22.42042	(0.88658)		
Sig. T	(0.0000)	(0.0000)			

[a] The second value in each set of R^2 is adjusted R^2.

Note: L-W joins = number of land-water joins.
ADJ-1 = number of water pixels bordered on one side by another water pixel.
ADJ-2 = number of water pixels bordered on two sides by other water pixels.
ADJ-3 = number of water pixels bordered on three sides by other water pixels.
ADJ-4 = number of water pixels bordered on four sides by other water pixels.